Atmospheric
Chemistry
and Physics
Discussions

Observed decreases in on-road CO_2 concentrations in Beijing during COVID-19

Di Liu[1], Wanqi Sun[2], Ning Zeng[3,4,], Pengfei Han[1*], Bo Yao[2, *], Zhiqiang Liu[1], Pucai Wang[5], Ke Zheng[1], Han Mei[1], Qixiang Cai[1]

[1]Laboratory of Numerical Modeling for Atmospheric Sciences & Geophysical Fluid Dynamics, Institute of Atmospheric Physics, Chinese Academy of Sciences

[2]Meteorological Observation Centre, China Meteorological Administration, Beijing, China

[3]Department of Atmospheric and Oceanic Science, University of Maryland, USA

[4]Earth System Science Interdisciplinary Center, University of Maryland, USA

[5]Laboratory for Middle Atmosphere and Global Environment Observation, Institute of Atmospheric Physics, Chinese Academy of Sciences

Correspondence to: Pengfei Han (pfhan@mail.iap.ac.cn); Bo Yao (yaob@cma.gov.cn)

Abstract:

To prevent the spread of the COVID-19 epidemic, restrictions such as "lockdown", were conducted globally, which led to significant reduction in fossil fuel emissions, especially in urban regions. However, CO_2 concentrations in urban regions are affected by many factors, such as weather and background CO_2 fluctuations. Thus, it is difficult to directly observe the reductions in CO_2 concentrations with sparse ground observations. Here, we focus on urban ground transportation emissions, which were dramatically affected by the prohibitions, to determine the reduction signals. We conducted six on-road CO_2 observations in Beijing using mobile platforms before (BC), during (DC) and after COVID-19 prohibitions (AC). To reduce the weather and background impacts, we chose trips with the most similar weather as possible and calculated the enhancement, which mean the difference in the CO_2 concentration between on-road and the "background" level measured at the Institute of Atmospheric Physics, Chinese Academy of Sciences (IAP) tower. The results showed that DC CO_2 enhancement decreased by 41 parts per million (ppm) and 26 ppm compared to those during BC and AC, respectively, after eliminating the fluctuations in CO_2 concentrations on polluted days. Detailed analysis showed that, during COVID, there was no difference between weekdays and weekends. The enhancements during rush hours were almost twice those during working hours, indicating that emissions during rush hours were much higher. Compared with DC and BC, the reductions in the enhancements during rush hours were much larger than those during working hours. Our findings showed a clear decrease during COVID, which are consistent with the CO_2 concentration and emissions reductions due to the pandemic. The enhancement way used in this study is an effective method to reduce the impacts of weather and background fluctuation and should be regularly and more frequently conducted in future work.

35   **Introduction:**

Since December 2019, the world has been fiercely struggling against a pandemic of a novel Coronavirus named COVID-19, which was firstly identified in Wuhan, China(Gross et al., 2020); and then quickly identified by other countries in east Asia, Europe and the United States(Le Quere et al., 2020). In Beijing, the first case was confirmed on 20th January 2020, and followed by a quick increase in confirmed cases (Figure 1A). From 24th January to 30th April, Beijing enacted a Level-1

40   response to major public health emergencies (red region, in Figure 1), and lowered the response to Level-2 from 30th April to 6th June, after "zero growth" persisted for almost one month (yellow region, in Figure 1).

As the world faced this highly infectious pandemic without efficient medication, governments carried out similar prohibitions to prevent the spread of the virus: isolating cases, enacting stay at home orders, forbidding mass gathering, and

45   closing factories and schools. These prohibitions highly altered the factory production, energy consumption and transportation volume and led to sharp emissions reductions (Liu et al., 2020;Le Quere et al., 2020). As previous inventory studies estimated, the global daily CO_2 emissions decreased by 17% (11 to 25% for $\pm 1\sigma$) by early April 2020 compared with the mean 2019 levels, and the absolute reduction was approximately 1048 (543 to 1,638) $MtCO_2$ until the end of April(Le Quere et al., 2020). Among these emissions, emissions from ground transportation obviously decreased by 36% (28 to 46)

50   (Le Quere et al., 2020). According to Liu *et al.(Liu et al., 2020)*, emissions decreases in China were 6.9% from January to April 2020, in which ground transportation emissions dropped abruptly by 53.4% in February and continued to decrease by 25.9% in March (Figure 1B and 1C). In Beijing, during the first quarter in 2020, passenger traffic volumes decreased 55.6%, and ground transport volumes decreased 35.2% according to the distance-weighted passenger and freight turnover(Han et al., 2020).

55

Although urban areas are the main CO_2 sources and account for more than 70% of fossil fuel emissions (Rosenzweig et al., 2010), the CO_2 concentration in urban area is dominated by weather changes (Woodwell et al., 1973;Grimmond et al., 2002). In addition, the absolute carbon emission reductions (258 MtC, from Le Quere *et al.*(Le Quere et al., 2020)) due to COVID was relatively small compared to the CO_2 content in the atmosphere (860 GtC, from Friedlingstein *et al.*(Friedlingstein et al.,

60   2019)), carbon uptake by vegetation (the average seasonal amplitude of the net land–atmosphere carbon flux is 41.6 GtC/yr, from Zeng *et al.*(Zeng et al., 2014)). Therefore, it is very difficult to detect a decrease in the urban CO_2 concentration decrease directly by sparse ground observations. For example, according to the daily CO_2 concentrations in 2019 and 2020 recorded by the Institute of Atmospheric Physics, Chinese Academy of Sciences (IAP) tower, even though Beijing was within the strictest control/confinement period from 10th to 14th February 2020, stable weather (poor diffusion conditions) led

65   to CO_2 concentrations that were approximately 90 parts per million (ppm) higher than those on the same date in 2019 (Figure 1D). Sussmann and Rettinger (2020) also proved it. Although global emissions reduction due to COVID-19, they found a historic record high in column-averaged atmospheric carbon dioxide (XCO2) in April 2020 by using Total Carbon Column Observation Network (TCCON) data. Assuming a COVID-19-related CO_2 growth rate reduction of 0.32 ppm/yr^2 in 2020 for Mauna Loa to be true and measured (from UK Met Office, overall 8% emissions reduction in 2020), they found there is ~0.6

70   yr 'delay' to separate TCCON-measured growth rates and the reference forecast (without COVID-19).

With the knowledge that urban ground transportation was strongly suppressed due to COVID, we designed on-road observations by using a mobile platform to find reduction signals. On-road observations based on mobile platforms, which could provide higher spatiotemporal resolution CO_2 data than satellite and ground observations, have been widely conducted

75   for carbon monitoring in urban and sub-urban regions (transects or communities)(Idso et al., 2001;Bush et al., 2015;Sun et al., 2019). However, all studies explained that weather (for example, wind speed which is directly associated with the diffusion condition) is a dominant factor and should be considered during analysis. However, it is still a problem to reduce the impact of weather. On the other hand, the enhancement, which calculates the difference in the CO_2 concentration between urban and rural background observations, could effectively reduce the influence of background CO_2 concentration

80   fluctuations to analyze CO_2 concentration characteristics in urban areas and has been widely used for monitoring urban carbon emissions and CO_2 concentration(Idso et al., 1998;Idso et al., 2002;George et al., 2007;Mitchell et al., 2018;Perez et al., 2009).

To determine the CO_2 concentration reduction "signal" due to ground transportation emissions decrease during COVID-19,
85   we first chose the most similar weather condition as possible; second, we calculated enhancements by using on-road CO_2 observations minus the "baseline" IAP tower CO_2 concentration to reduce the influence from the fluctuation in the background CO_2 concentration due to weather. Our results may provide direct evidence of ground transportation emission reductions due to COVID-19, and this method could be an appropriate tool to analyze the CO_2 concentration and emissions of urban ground transportation in the future works.
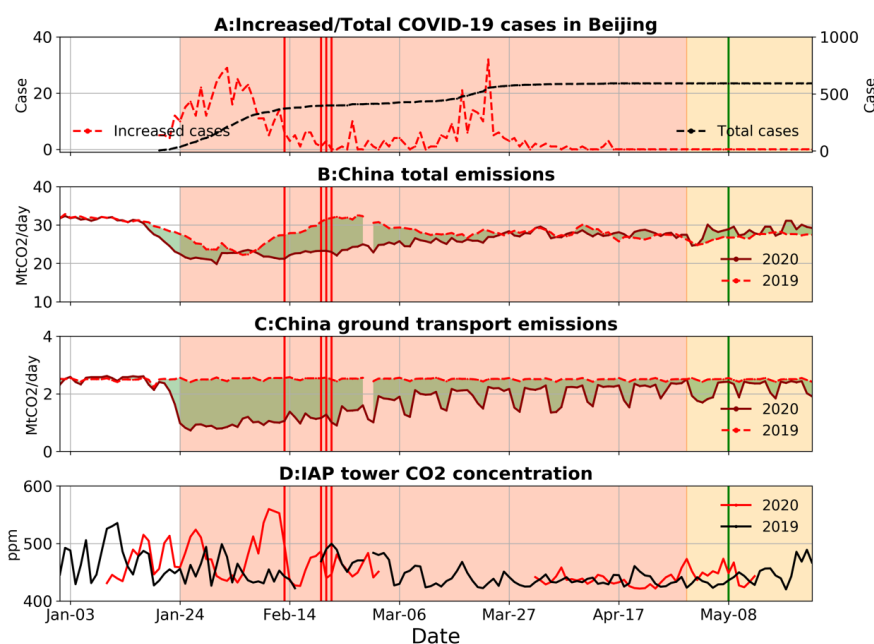
90

Figure 1. (A) Confirmed increased cases (red) and total cases (black) of COVID-19 in Beijing in 2020; the red/yellow region is the Level-1/2 response periods; vertical lines indicate the on-roads observation dates, red/green lines indicate during and after COVID, respectively. One trip was conducted on 20th February 2019, which was not plotted in Figure 1. (B) China
95   *daily CO_2 emissions in the five months of 2019 (dotted line) and 2020 (solid line), data from Liu et al. (Liu et al., 2020). (C) China ground transport daily CO_2 emissions in the first five months of 2019 and 2020, data from Liu et al.(Liu et al., 2020). (D) Comparison of IAP tower CO_2 concentrations in 2019 (black) and 2020 (red).*

Methods and Data:

100   We conducted six on-road observations in Beijing using mobile platforms before (BC; 1 trip: 20th February 2019), during (DC; 4 trips: 13th, 20th, 21st and 22nd February 2020) and after (AC; 1 trip: 9th May 2020) COVID-19 control (vertical lines in Figure 1 indicate trip dates). These trips covered the four ring roads that circle the city, which are the 2nd (with length of 32.7 km), 3rd (48 km), 4th (64 km) and 5th (99 km) Ring Roads from innermost to outermost, as shown in Figure 2. All trips were

conducted during the daytime, in which four of them were on weekdays and others were on Saturday. Four trips covered at
105   least one rush hour.

To reduce the background fluctuations, we first chose the similar weather conditions. Three elements were considered: (1)
reality photos collected from the IAP tower (photo available from: http://view.iap.ac.cn:8080/imageview/); (2) the $PM_{2.5}$
(atmospheric particulate matter that has a diameter of less than 2.5 μm) concentration from the Olympic Sports Center
110   Station (40.003 °N, 116.407 °E, 5 m height, purple square in Figure 2A), which is run by the Ministry of Ecology and
Environment of China(Zhang et al., 2015); (3) and wind speed data (available collected from:
https://www.wunderground.com/history/daily/cn/beijing/ZBNY/date/2020-5-9).

Then, on-road CO_2 concentration enhancements were calculated by subtracting the simultaneous CO_2 concentrations from
115   the IAP tower, which implies the "baseline" in Beijing city (Eq. 1).

$$CO_2 \text{ enhancement} = CO_2 \text{ (on-road)} - CO_2 \text{ (IAP tower)} \qquad \text{(Eq. 1)}$$
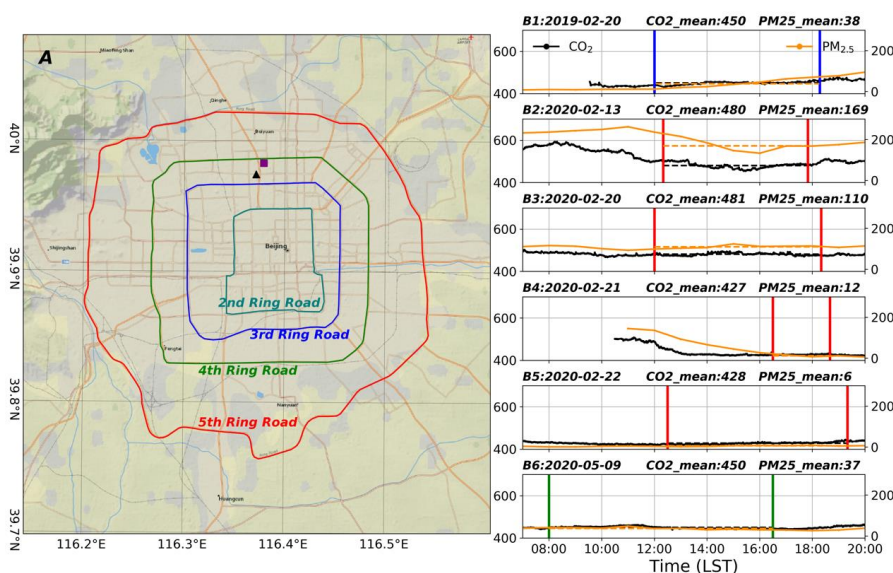
Figure 2. A: The locations of the 2nd, 3rd, 4th and 5th Ring Roads, the IAP tower (black triangle) and Olympic Sports Centre
120   station (purple square); B1-B6: CO_2 concentration from the IAP tower and $PM_{2.5}$ data from the Olympic Sports Center
station during six trips.

Table 1. Weather conditions during six trips.

Label/date	Weather condition	Air condition (PM2.5: μg/m³)	Wind speed (m/s)	Reality photos
BC 2019-2-20 (Wed)	Clear day	38	2.5	

DC 2020-2-13 (Fri)	Light polluted day	169	2.5	
DC 2020-2-20 (Fri)	Light polluted day	110	1.3	
DC 2020-2-21 (Fri)	Clear day	12	2.5	
DC 2020-2-22 (Fri)	Clear day	6	3.6	
AC 2020-5-9 (Sat)	Clear day	37	1.6	

IAP tower CO_2 concentration data:

125   The IAP tower is a 325 m high meteorological tower located at 116.3667 °E, 39.9667 °N, 49 m above sea level in northwest Beijing (Figure 2, black triangle). There are three levels of CO_2 concentration records: surface level (~2 m above ground), lower level (~80 m) and upper level (~280 m)(Cheng et al., 2018). The CO_2 concentrations were measured by a Picarro G2301 greenhouse gas concentration analyzer(Picarro, 2019).The instrument is calibrated every 3 hours by using standard

130   gas from the Meteorological Observation Center of China Meteorological Administration (MOC/CMA), which is traced to the World Meteorological Organization (WMO) X2007 scale, and each calibration lasts for 5 minutes. The measurement precision is ~0.1 ppm. All CO_2 concentrations were recorded by every 2 seconds and then averaged into 1-minute intervals. Before 2020 (including the trip on 20th February 2019), the CO_2 concentrations were measured at the lower and upper levels alternately for every 5 minutes, and each level lasted 5 minutes. After 2020 (including the other 5 trips), the CO_2

135   concentration was continuously measured at the surface level. To maintain consistency as much as possible, we used the lower level CO_2 concentrations before 2020 and surface levels after 2020.

On-road CO_2 concentration data:

Atmospheric
Chemistry
and Physics
Discussions

Three different CO_2 observation instruments were carried by vehicles for six on-road trips (Table 2).

140   1)   On 20th February 2019, a Picarro G2401(Picarro, 2017) was adopted and installed on a vehicle; the air intake was set on the roof of the vehicle to avoid potential direct plumes emitted from surrounding cars. The intake was linked/connected through a 2 m pipe with a particulate matter filter to Picarro (Figure 3A and 3B). The instruments characteristics and precision have been described by Sun *et al.*(Sun et al., 2019). The CO_2 concentrations were collected every 2 seconds and then averaged into 1-minute intervals.

145   2)   During COVID-19 (surveys on 13th, 20th, 21st and 22nd February 2020), a LI-COR LI-7810 CH_4/CO_2/H_2O trace gas analyzer was adopted, which uses optical feedback-cavity enhanced absorption spectroscopy technology(LI-COR, 2019). This instrument could obtain a CO_2 concentration with a precision of 3.5 ppm for 1 second and within 1 ppm after 1-minute averaging (lab testing). The observation platform of the LI-7810 was similar to that of Picarro. Before departure, the instrument was calibrated by using standard calibration gas (from MOC/CMA) to correct the drift.

150   3)   On 9th May 2020, a low-cost light sensor was adopted and installed on the front windshield of the vehicle (Figure 3C). The instrument mainly consisted of three non-dispersive infrared (NDIR) CO_2 measurement sensors (named K30), and one environment (temperature, humidity and pressure) sensor (named BME). Although the original precision of each K30 is ±30 ppm, after calibration and environmental correction in the lab, it was improved to within ±5 ppm comparing with Picarro(Martin et al., 2017;SenseAir, 2019). Here, we used three K30s in one instrument to recognize and 155   eliminate data anomalies and used the averaged CO_2 concentrations from the three K30s for analysis. Figure 4 shows the experiment conducted on 22nd February 2020, which installed one low-cost light sensor and Picarro on the same vehicle for on-road monitoring. The results showed that the low-cost light sensor results are highly consistent with those of Picarro, with root mean square errors (RMSEs) less than 5 ppm.

160   *Table 2. Instrument parameters of six on-road observations*

Label	Date	Instrument	Precision	Temporal resolution (original->processed)
BC	2019-2-20	Picarro G2401	0.1 ppm	2 seconds -> 1 minute
DC	2020-2-13	LI-COR LI-7810	±3.5 ppm (for 1 second); improved into 1 ppm for 1 minute	1 second -> 1 minute
	2020-2-20	LI-COR LI-7810		
	2020-2-21	LI-COR LI-7810		
	2020-2-22	LI-COR LI-7810		
AC	2020-5-9	Low-cost Sensor (K30)	±5 ppm	2 seconds -> 1 minute
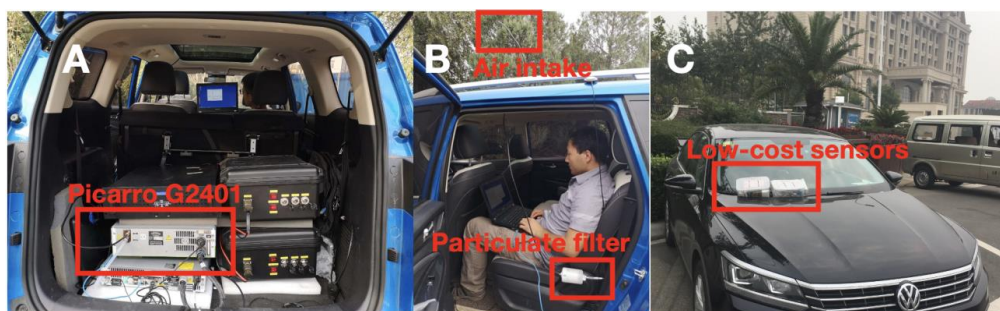
Figure 3. Photos of instrument installation during on-road observations. (A) and (B) Picarro installed in the vehicle; (C) 165   *low-cost non-dispersive infrared (NDIR) sensors installed on the front windshield of the vehicle.*
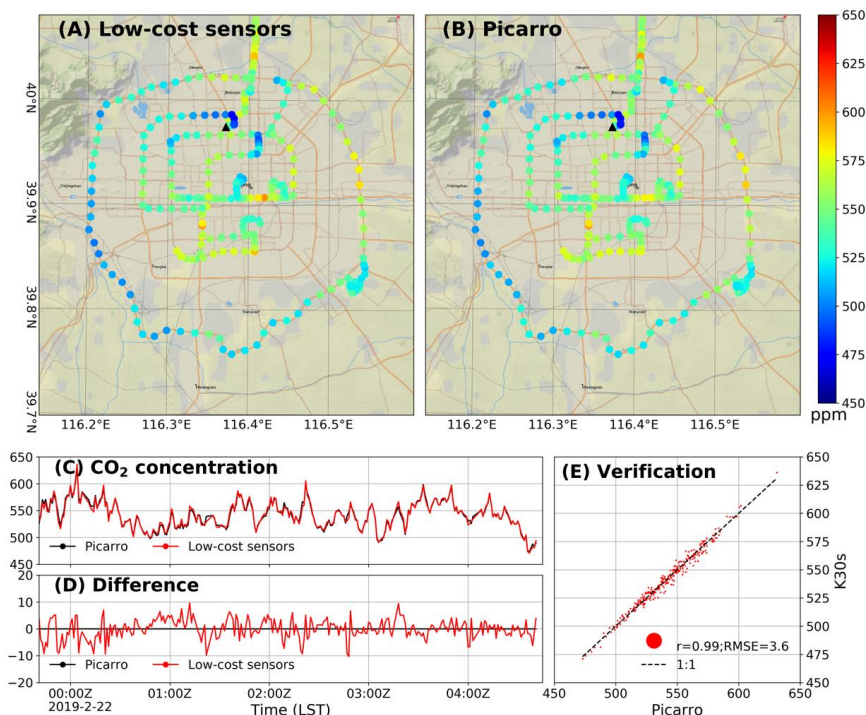
Figure 4. Verification of low-cost sensors for on-road observations. (A): CO$_2$ concentration map of the low-cost sensor; (B): CO$_2$ concentration of Picarro on the same vehicle; (C): time series of CO$_2$ concentration by using the low-cost sensor and Picarro; (D): difference (low-cost sensor minus Picarro); (E): scatter plot of the low-cost sensor and Picarro, with a RMSE of 3.6 ppm.

Auxiliary data and analysis:

The global positioning system (GPS) data during BC and DC were collected by a GPS receiver (BS-70DU)(Sun et al., 2019). During AC, the data were collected by using mobile software (GPS Tracks), which provided time, longitude, latitude, speed and altitude at 1 second resolution. These geographic information data were averaged into 1-minute intervals and then matched with CO$_2$ concentration data according to time.

Two remote sensing images were adopted (captured on 21st February 2019 at 11:40:00 Local Standard Time (LST), from a Google Earth image, with 0.37 m spatial resolution; 19th February 2020 at 10:20:08 LST, from a Beijing-2 remote sensing satellites panchromatic image, with 0.8 m spatial resolution). Considering the availability of data, we used the images from the closest date and only part of the urban area. The comparison region covered 13.4 km of the 4th Ring Road (accounting for 20.5 % of the whole road, for which the total length is 65.3 km) and 10 km of the 3rd Ring Road (accounting for 20.7 % of the whole road, for which the length is 48.3 km). We used a visual interpretation method to obtain the numbers of vehicles on the 4th and 3rd Ring Roads before and during the COVID-19, respectively.

Results:

On-road CO$_2$ concentration:
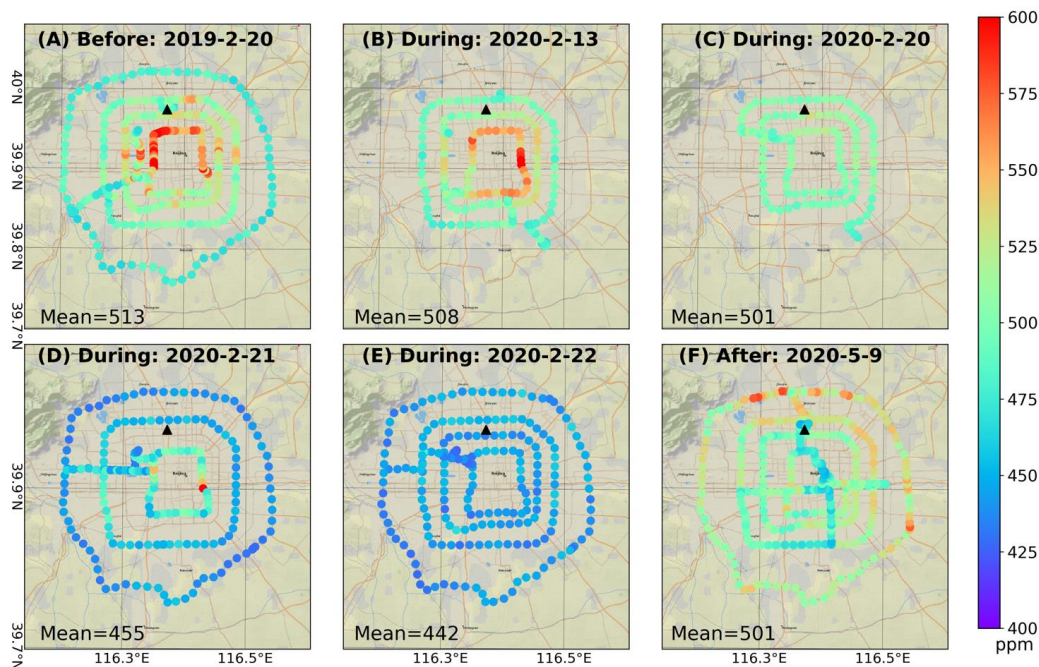
Figure 5. CO_2 concentration maps of six on-road trips. Circle points are the locations of CO_2 concentration records at the 1-minute intervals averaged from data collected every 2 seconds (see methods). All sub-plots have the same color bar, ranging from 400 to 600 ppm. The black triangle is the location of the IAP tower. One trip (A:20th February 2019) was conducted before the COVID-19 control, with an average of 513 ppm. Four trips (B-E: 13th, 20th, 21st and 22nd February 2020) were conducted within the COVID-19 control, and the total average CO_2 was 477 ppm. One trip (F: 9th May 2020) was conducted after the COVID-19 control, with an average of 501 ppm.

The CO_2 concentration maps of six on-road trips are shown in Figure 5. One trip was chosen as an example for BC (on 20th February 2019), DC (21st February 2020) and AC (9th May 2020) (shown in Figure 5A, 5D and 5F). All three trips were conducted on clear days, and their trajectories were similar that from the outermost circle to the innermost circle and covered one (morning or evening) rush hour. The difference was that the BC and DC trips hit the evening rush hour on the innermost circle road, whereas the AC trip hit the morning rush hour on the outermost circle. This difference explained the CO_2 concentration patterns (Figure 5A, 5D and 5F). The comparison of the three trips indicated that the CO_2 concentration measured in Figure 5D was intuitively lower than that in Figure 5A and 5F, and the statistics show that the DC CO_2 mean was approximately 58 and 46 ppm lower than that of the BC and AC trips, respectively. In addition, the average CO_2 concentration observed by the IAP tower during the same periods was much lower than the on-road observations (Figure 2). These concentration differences (gradients) also implied that ground transportation emissions were a major CO_2 source on urban roads.

The other three DC trips (on 13th, 20th and 22nd February 2020) are shown in Figure 5B, 5C and 5E, with the averaged CO_2 concentrations of 508, 501 and 442 ppm. Due to background CO_2 concentration fluctuations (lightly polluted days), CO_2 concentrations on 13th and 20th February (Figure 5B and C) were as high as those during the BC and AC trips. Statistically, without considering the variation in the background CO_2 concentration, the average of the four DC trips was 477 ppm, which was 36 and 24 ppm lower than that of the BC and AC trips, respectively.

215 **On-road CO$_2$ enhancement:**
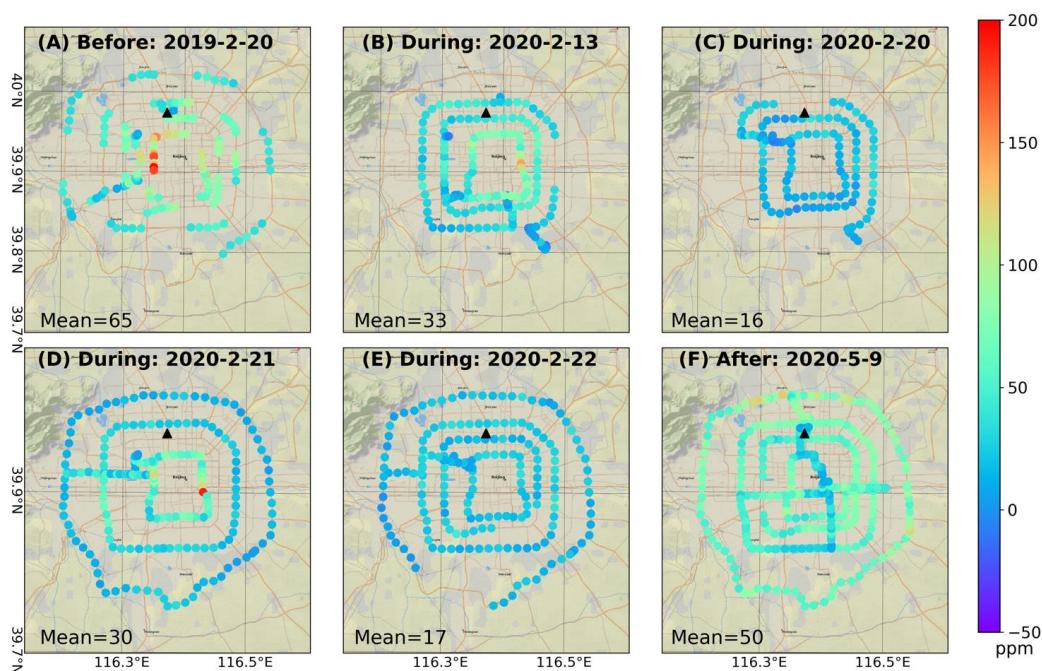
Figure 6. CO$_2$ enhancement maps of all six trips using on-road CO$_2$ minus IAP tower measurements matched by time. All sub-plots have the same color bar, ranging from -50 to 200 ppm. One trip (A:20th February 2019) was conducted before the COVID-19 control with an average of 65 ppm. Four trips (B-E: 13th, 20th, 21st and 22nd February 2020) were conducted

220 *within the COVID-19 control, and the total averaged CO$_2$ enhancement was 24 ppm. One trip (F: 9th May 2020) was conducted after the COVID-19 control with an average of 50 ppm.*

Figure 6 shows the CO$_2$ enhancement maps of six trips, using the on-road CO$_2$ concentration minus those of IAP tower at the same time. The enhancements present a refined spatial distribution of the CO$_2$ concentration gradient, which implies ground

225 transportation CO$_2$ emissions. As an example, Figures 6A, 6D and 6F presents the BC, DC and AC enhancement maps, respectively. Statistics show that enhancement during the DC trip was 30 ppm, which is 35 and 20 ppm lower than that before and after this trip. The spatial distribution patterns of enhancement were similar to the CO$_2$ concentration maps, in which enhancements during rush hours were much higher for all trips. Compared to the CO$_2$ concentration maps, the enhancements showed important information in Figure 6B and 6C. The averaged CO$_2$ concentrations in these two trips were

230 similar to those during BC and AC (Figure 5B and 5C); however, the enhancements that extracted traffic emission signals from the background, with averages of 33 and 16 ppm (Figure 6B and C), were much lower than those of BC and DC. The enhancement maps also showed more useful information than the CO$_2$ concentration maps. For example, although the CO$_2$ concentration throughout the northern half of the 2nd Ring Roads was high (550~600 ppm) (Figure 5A), the enhancement extracted more specific variations induced by traffic emissions in the northwest (Figure 6A). Generally, the statistical

235 enhancement the average of the four DC trips was 24 ppm, which was 41 and 26 ppm lower than that of the BC and AC trips, respectively. Because of the IAP tower Picarro calibration and measurement procedure (see Method Section), there were regular data gaps for the trip on 20th February 2019 (Figure 6A).

Diurnal variation analysis:
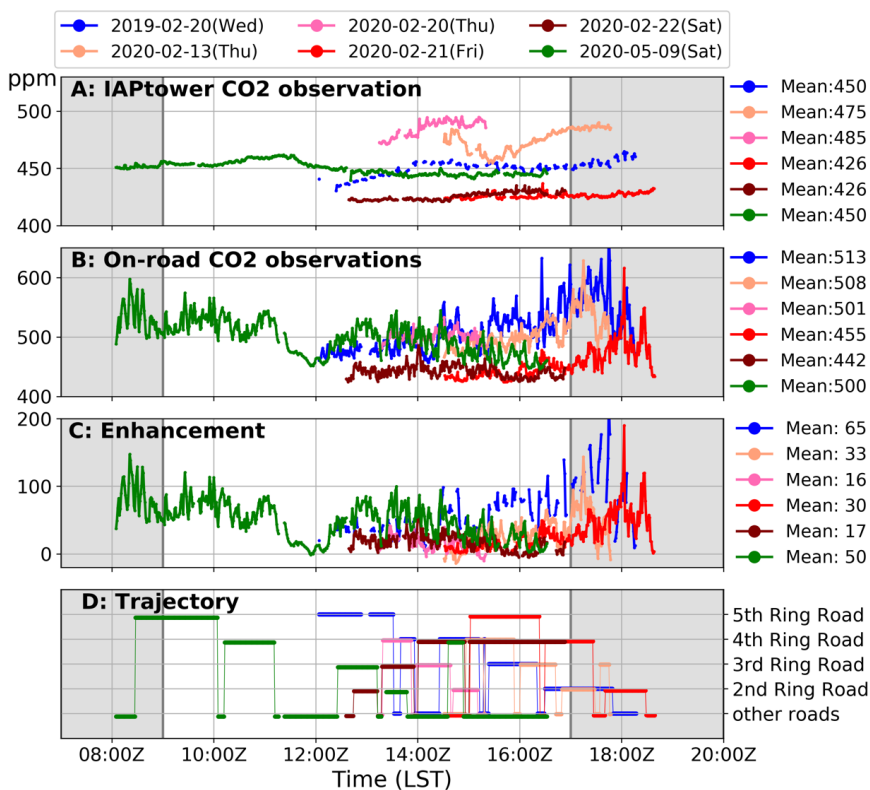
Figure 7. Six trips were plotted on a single day. The two grey regions refer to morning and evening rush hours. The six colorful lines represent the six trips on different days. Four of the 6 trips covered at least one (morning/evening) rush hour. Panel A shows the CO_2 concentration from IAP tower during the trips. Panel B shows the on-road CO_2 concentration. Panel C shows the CO_2 enhancements. Panel D shows the six trip trajectories.

Figure 7 shows the diurnal variation from the IAP tower CO_2 concentrations, on-road CO_2 concentrations, enhancements and trajectories for all trips. In Figure 7A, the IAP tower CO_2 concentrations were relatively stable, and showed the difference between trips. The CO_2 concentrations during the two trips during COVID-19 (13th and 20th February 2020) were ~30 ppm higher than those during the BC and AC trips. However, the CO_2 concentrations during the other two trips (21st and 22nd February 2020) were ~20 ppm lower than those during the BC and AC trips. These "baseline" CO2 concentration fluctuations make the on-road observations not comparable directly. In Figure 8B, the CO_2 concentrations show a "double-peak" pattern within the morning (7:00-9:00) and evening rush hours (17:00-20:00). During the rush hours, the CO_2 concentrations ranged from 500 to 600 ppm, which were approximately 100 ppm higher than the concentrations during working hours (9:00-17:00). The comparison of BC and AC indicates that the CO_2 concentrations measured on 13th and 20th February 2020 did not significantly decrease during 12:00-17:00. However, the CO_2 concentrations measured on 21st and 22nd February 2020 were much lower (~50 ppm) than those measured during the BC and AC trips. This difference is consistent with the spatial distribution mentioned before and is most likely due to the CO_2 concentration background fluctuations.

In Panel C, all DC CO_2 enhancements were generally lower than those of BC and AC. However, we still found very low enhancements values for BC and AC; for example, AC enhancement at approximately 12:00 and 16:00 was almost the same as that of DC. With the help of trip routes (Panel D), we found that during that period, the on-road observation vehicle was

not driving on the main ring roads. Another example is BC at approximately 18:00, which indicates that the enhancement decreased in a stepwise manner, also because the vehicle drove on other roads (Panel D). In Panel C, all DC CO_2 enhancements were generally lower than those of BC and AC, and the statistics for different time periods are also listed in Table 3.

265

Table 3. Statistical analysis of CO_2 enhancement for six trips (ppm)

Label	Observation date	Weather condition	Total average (07:00-20:00)	Morning RUSH hours (07:00-09:00)	Working hours (09:00-17:00)	Evening RUSH hours (17:00-20:00)
BC	2019-2-20 (Wed)	Clear	65	-	54	100
	2020-2-13 (Thu)	Stable/light pollution	33	-	26	55
DC	2020-2-20 (Thu)	Stable//light pollution	16	-	16	-
	2020-2-21 (Fri)	Windy day	30	-	16	50
	2020-2-22 (Sat)	Windy day	17	-	17	-
AC	2020-5-9 (Sat)	Windy day	50	80	46	-
	Total BC-DC		41	-	35	48
	Total AC-DC		26	-	27	-

270

The average of CO_2 enhancement for the whole BC trip was 65 ppm, and the average for the evening rush hour (100 ppm) was two times that of the working hours (54 ppm). This result implies that the increase in vehicle volume in the evening rush hours leads to large traffic emissions and an increase in the on-road CO_2 concentration. For DC, all trips covered the working hours, with a low enhancement of approximately 20 ppm. There was not obvious difference between weekdays and

275   weekends during this period, which indicated that there was no "week effect". The reason may because the government encouraged people to work remotely at home. Therefore, even on weekdays, the commute was small. Among these four trips, two (13th and 20th February 2020) covered the evening rush hours with high averaged enhancements of 55 and 50 ppm. Therefore, the total enhancement averages of these two trips were higher than those of the other two trips, which covered only working hours. For AC, on 9th May 2020, although it was a Saturday, many residents chose to go out of town for

280   weekends. The morning rush hours still existed, with a high enhancement of 80 ppm, and then during the working hours, the enhancement decreased to 46 ppm.

The comparison of trips showed that the averaged CO_2 enhancement from 4 whole DC trips was 41 and 26 ppm lower than that from the BC and AC trips, respectively. Compared to the BC trip, the averaged AC enhancement was 15 ppm lower.

285   This difference may be caused by two factors: 1) "weekly effects", as previously mentioned; a previous study also suggested that, compared to weekdays, the average daily traffic CO_2 emissions during weekends in the north part of the fifth Ring Road

(LinCui Road - Anli Road, 3 km) decreased by 5% throughout whole 2014 according to the Motor Vehicle Emission Simulator model (from 131.74 t/d to 126.33 t/d)(Zheng et al., 2020); 2) until 9th May 2020, although there were approximately 30 days without increased COVID-19 cases in Beijing, the city was still under Level-2 response control; social life was recovering, but had not yet completely recovered.

Analysis of CO_2 enhancement on independent time periods and roads:

According to the previous analysis, we found that enhancement exhibited a strong correlation with the time (rush or working hours) and road types. Therefore, we statistically analyze CO_2 enhancements according to road types and time periods, as shown in Figure 8. In Figure 8A, on 13th and 20th February 2020, the CO_2 concentrations on the other, 2nd, 4th Ring Roads and all roads were at the same levels as those during the BC and AC trips. However, in Figure 8B, the enhancement showed that the four trips during COVID-19 were generally lower than those during AC and BC for all road types. Although on the 2nd Ring Road, the DC trips on 13th and 21st February 2020 were almost the same as the BC and AC trips, the DC trips were during rush hours, whereas the AC and BC trips were during working hours. Some very high deviations also occurred (rush hours on the other roads, 2nd and 5th Ring Roads), which indicates the dispersion of CO_2 enhancement. The reason for this difference is that we classified all roads excluding the ring roads as other roads, which may include arterial and residential roads, so the different road types may increase the deviation. For the 2nd and 5th Ring roads, high deviation occurred because during rush hour, traffic flow and transportation vary greatly and result in drastic changes to CO_2 enhancement, which also causes much higher deviations. We also calculated specific statistics, which are listed in Table 4.
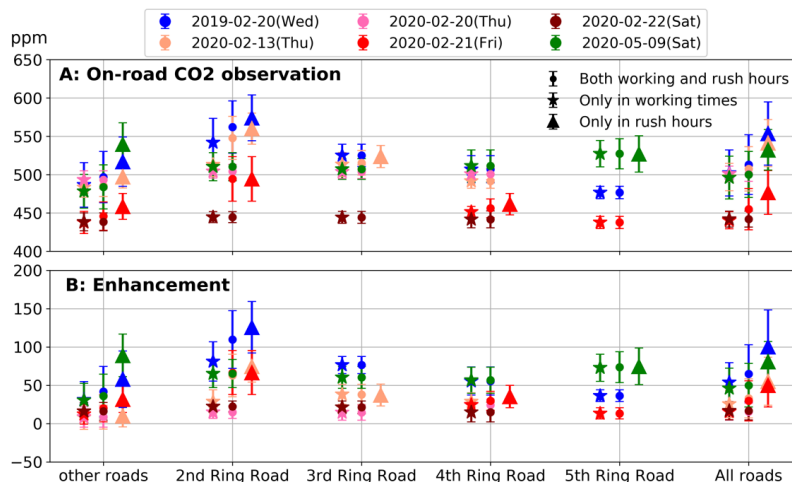

Figure 8. Statistically analysis of all on-road trips according to road types and times. Panel A shows the on-road CO_2 concentration. Panel B shows the CO_2 enhancement.

Table 4. Statistical analysis of CO_2 enhancement for six trips according to times and roads

Label	date	Time	other roads	2nd Ring Road	3rd Ring Road	4th Ring Road	5th Ring Road	All roads
BC	2019-2-20 (Wed)	Working hours	31±24	81±26	77±11	56±18	37±8	54±26
		Rush hours	58±37	125±34	-	-	-	100±48
		Both	42±33	109±38	77±11	56±18	37±8	65±38

Group	Date	Period						
DC	2020-2-13 (Thu)	Working hours	8±16	29±15	38±13	29±11	-	26±18
		Rush hours	10±14	74±20	37±14	-	-	55±31
		Both	9±16	63±28	38±13	29±11	-	33±26
	2020-2-20 (Thu)	Working hours	9±13	15±8	14±10	24±8	-	16±11
		Rush hours	-	-	-	-	-	-
		Both	9±13	15±8	14±10	24±8	-	16±11
	2020-2-21 (Fri)	Working hours	12±13	-	-	25±7	13±7	16±10
		Rush hours	32±17	67±29	-	35±15	-	50±28
		Both	20±18	67±29	-	30±13	13±7	30±26
	2020-2-22 (Sat)	Working hours	16±11	22±7	21±8	15±13	-	17±12
		Rush hours	-	-	-	-	-	-
		Both	16±11	22±7	21±8	15±13	-	17±12
AC	2020-5-9 (Sat)	Working hours	30±22	65±18	60±14	57±17	73±18	46±26
		Rush hours	89±28	-	-	-	75±24	81±26
		Both	36±29	65±18	60±14	57±17	73±20	50±28

310

Discussion:

Correlation analysis with traffic flow：

It was difficult to obtain a quantitative evaluation of the influence of COVID-19 on CO_2 emissions from traffic during our study period because there were limited data. In this study, we found one trip enhancement during DC (on 21st February 2020, with the most similar weather and route as trips during BC and AC) was 30 ppm. The enhancement accounted for 46% of that during BC (65 ppm), and the enhancement during AC (50 ppm) account 77% of that during BC. Here, we adopted four data and methods to explain our hypothesis that the decrease in traffic volume led to a reduction in on-road CO_2 emissions and concentration during COVID-19 control. First, according to "analysis of road traffic operation in Beijing during COVID-19 in 2020" published by the Beijing Transport Institute, during the first 8 weeks (from 1st February to 31st March, DC period in this study), Beijing ground transportation index (calculated based on ratio of congestion road length and whole road length) decreased by 53% compared to normal days; whereas, during 1st April to 31st May, the index recovered to 92%(Zhang, 2020). The index implied that traffic flow of DC is dramatically decreased compared to that of BC, and AC recovered almost but not completely. This index variation is consistent with our observations results. Second, two remote sensing images from similar dates were adopted (Figure 9). According to statistics and estimations based on coverage area, we found that the BC traffic flows on the main roads of the 4th and 3rd Ring Roads are 227 and 226 veh/km (vehicles per kilometer), respectively. However, the DC traffic flow decreased to 35 and 34 veh/km, with a reduction of approximately 85%. Simply assuming that emission factors were the same, the CO_2 emissions on roads during DC may have sharply decreased by approximately 85% compared to those during BC. This difference is higher than the passenger transportation decrease estimated by Han *et al.*'s(Han et al., 2020) (55.6% in the first quarter of 2020) because the remote sensing image is a snapshot and part of the urban area, and Hans' results are the average of the first three months and the entire Beijing administrative region. Third, we also collected real-time traffic congestion conditions (for each road), road name, geographic

13

information, road type and average speed for one-hour data from the Autonavi Open Platform (https://lbs.amap.com/). The
data, although with low temporal and spatial resolution, could be used to show traffic conditions on roads, and then indicate
the on-road traffic flow and emissions (Figure 10). Fourth, the vehicle speed maps of six trips were also plotted (Figure 11).

335   Overall, these maps reflect the spatial patterns of road traffic conditions during the surveys and could also reflect the
specifics on a single road. However, these maps are subject to subjective speed variations caused by drivers, such as when
facing traffic lights.
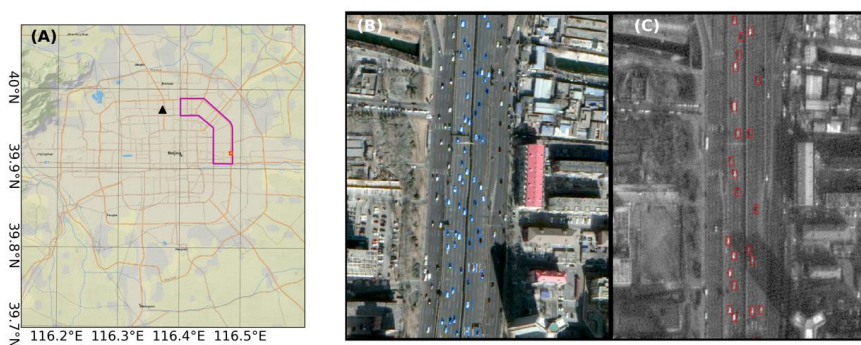
340   *Figure 9. Traffic volume comparison by using remote sensing images. (A) Coverage region of remote sensing images (purple polygon) and example region shown on the right (red square); (B) remote sensing images from Google Earth on 21st February 2019 at 11:42:00 (LST), with a spatial resolution of 0.37 m for multispectral band images; 61 vehicles on the main road were interpreted (labelled by blue polygons); (C) remote sensing image from Beijing-2 satellite on 19th February 2020 at 10:20:08 (LST), with a spatial resolution of 0.8 m for panchromatic band images and 24 vehicles labelled by red*

345   *polygons.*
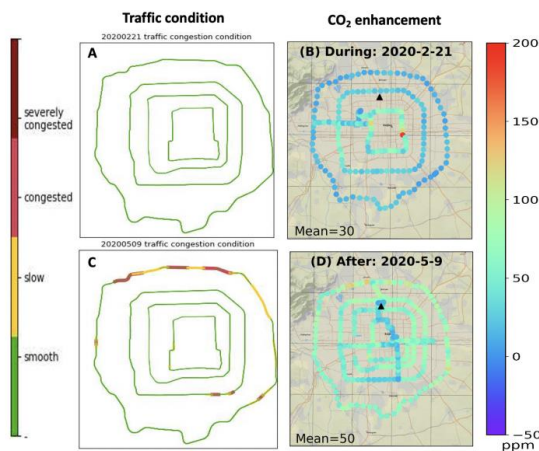
Figure 10. Traffic condition comparison with CO_2 enhancement. (A) Traffic conditions on 21st February 2020; (B) CO_2 enhancement on 21st February 2020; (C) traffic conditions on 9th May 2020; (D) CO_2 enhancement on 9th May 2020.
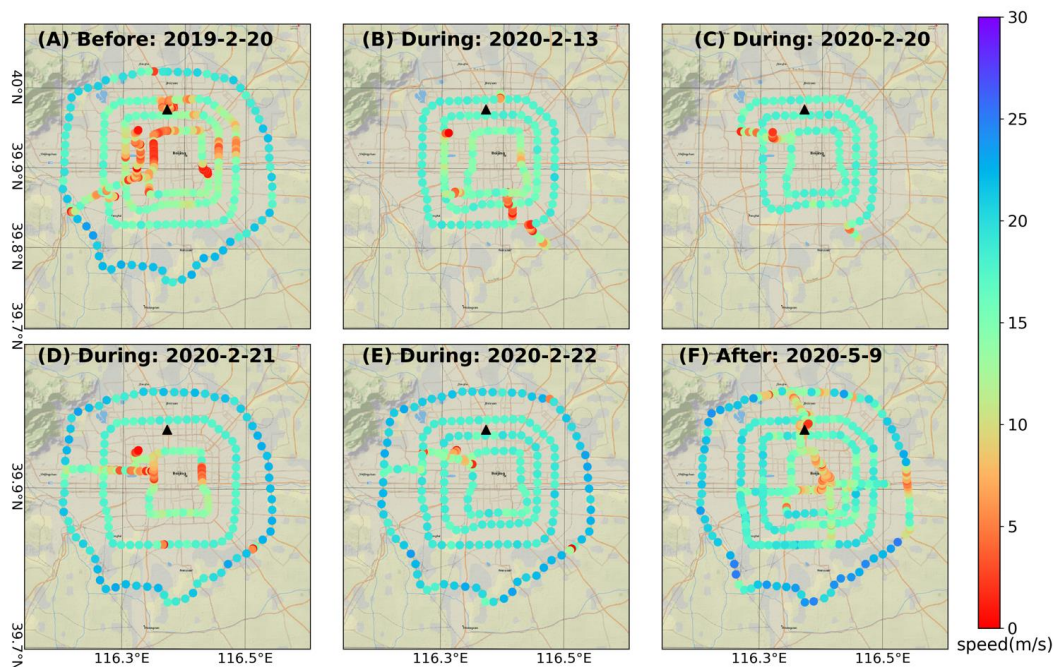
350

Figure 11. Speed maps of six trips, ranging from 0 to 30 m/s. One trip (A: 20th February 2019) was conducted before the COVID-19 control. Four trips (B-E: 13th, 20th, 21st and 22nd February 2020) were conducted during the COVID-19 control; one trip (F: 9th May 2020) was conducted after the COVID-19 control.

355

Uncertainty analysis:

The uncertainty of this research mainly existed in the following terms:

360 (1) The IAP tower CO_2 concentration was used as the background in Beijing.

In this study, IAP tower data were adopted as the urban background CO_2 concentration in Beijing. However, IAP tower data were collected from different levels, as described in the method section. Generally, high-level data would have a large footprint and cover large regions. For example, Cheng *et al.*(Cheng et al., 2018) showed that 280 m height-level CO_2 data have an averaged fetch of ~17 km, which may cover a major part of the city; 80 m height-level data have an averaged fetch

365 of ~8 km; and 8 m height-level data may have aa averaged fetch of only ~230 m, and the surface level (2 m) may be smaller. Due to the data availability and comparison consistency, we chose the lower and surface level data. According to Cheng *et al.*(Cheng et al., 2018), the CO_2 concentration at the 80 m height level is ~15 ppm higher than that at 8 m. Therefore, adding this difference between the lower level and surface level, the BC enhancement would increase (~15 ppm), which means that the DC enhancement would be even lower (~56 ppm) than the BC enhancement. This result is consistent with our

370 hypothesis.

(2) When data were collected, especially when switching between lower and upper levels, a large amount of data was lost. However, because the data gaps were evenly distributed and the IAP tower CO_2 concentrations were relatively stable, we assumed that it would not affect the final statistical results.

(3) In this study, our on-road observations did not have a fixed route or beginning/ending time, which means that the

375 observations on different dates represented different roads. Therefore, we analyzed a wide time range of observations (rush hours, working hours or whole day), which may also cause uncertainty.

Conclusion

The CO_2 emission reduction caused by COVID-19 is an opportunity to test our ability to collect CO_2 observations in urban regions. In this study, aiming at traffic emissions, which the potentially represents the largest reduction source in urban areas

380 due to COVID-19, we conducted six on-road observations in Beijing, China. The results showed that on-road CO_2 concentrations were strongly affected by traffic emissions and weather. However, the enhancement which was the difference of on-road CO_2 concentration and the city "background", reduced the impact of background CO_2 fluctuations. The results showed that during COVID-19, the total average CO_2 enhancements of the four trips were 41 ppm and 26 ppm lower than those before and after, respectively. Detailed analysis showed that this reduction commonly existed on all road types during

385 the same time period (rush hours/working hours). During COVID-19, there was no significant difference between weekdays and weekends. During rush hours, the enhancements were much higher than those during working hours, and compared with BC, the DC enhancements reduction during rush hours was most obvious. Our findings, which show a clear decrease during DC compared with those during BC and AC, are consistent with the COVID-19 control, which may be direct evidence of reductions in CO_2 concentrations and carbon emissions. On-road CO_2 observations are an effective way to understand and

390 analyze urban carbon CO_2 concentration distribution and variation and should be regularly and more frequently conducted in future work. With the development and successful application of miniaturized and low-cost CO_2 monitoring instruments used in this study(Khan et al., 2012;Shusterman et al., 2016;Martin et al., 2017;Mueller et al., 2020;Bao et al., 2020), these instruments will greatly help collect on-road observations and even high-density network observations and play a key role in future urban carbon observations.

395

Author contributions

Pengfei Han, Bo Yao and Ning Zeng conceived and designed the study. Di Liu summarized the results and wrote the draft of the paper. Wanqi Sun and Pengfei Han designed and conducted the on-road observations. Pucai Wang provided the IAP tower observation data. Ke Zheng, Zhiqiang Liu, Han Mei and Qixiang Cai helped to collect, process and analyze data.

400

Competing interests.

The authors declare that they have no conflicts of interest.

References:

Bao, Z., Han, P., Zeng, N., Liu, D., Cai, Q., Wang, Y., Tang, G., Zheng, K., and Yao, B.: Observation and modeling of vertical

410 carbon dioxide distribution in a heavily polluted suburban environment, Atmospheric and Oceanic Science Letters, 13, https://doi.org/10.1080/16742834.2020.1746627, 2020.

Bush, S. E., Hopkins, F. M., Randerson, J. T., Lai, C. T., and Ehleringer, J. R.: Design and application of a mobile ground-based observatory for continuous measurements of atmospheric trace gas and criteria pollutant species, Atmospheric Measurement Techniques, 8, 3481-3492, 10.5194/amt-8-3481-2015, 2015.

415 Cheng, X. L., Liu, X. M., Liu, Y. J., and Hu, F.: Characteristics of CO2 Concentration and Flux in the Beijing Urban Area, Journal of Geophysical Research-Atmospheres, 123, 1785-1801, 10.1002/2017jd027409, 2018.

Friedlingstein, P., Jones, M. W., O'Sullivan, M., Andrew, R. M., Hauck, J., Peters, G. P., Peters, W., Pongratz, J., Sitch, S., Le Quere, C., Bakker, D. C. E., Canadell, J. G., Ciais, P., Jackson, R. B., Anthoni, P., Barbero, L., Bastos, A., Bastrikov, V., Becker, M., Bopp, L., Buitenhuis, E., Chandra, N., Chevallier, F., Chini, L. P., Currie, K. I., Feely, R. A., Gehlen, M., Gilfillan, D.,

420 Gkritzalis, T., Goll, D. S., Gruber, N., Gutekunst, S., Harris, I., Haverd, V., Houghton, R. A., Hurtt, G., Ilyina, T., Jain, A. K., Joetzjer, E., Kaplan, J. O., Kato, E., Goldewijk, K. K., Korsbakken, J. I., Landschuetzer, P., Lauvset, S. K., Lefevre, N., Lenton, A.,

Lienert, S., Lombardozzi, D., Marland, G., McGuire, P. C., Melton, J. R., Metzl, N., Munro, D. R., Nabel, J. E. M. S., Nakaoka, S.-I., Neill, C., Omar, A. M., Ono, T., Peregon, A., Pierrot, D., Poulter, B., Rehder, G., Resplandy, L., Robertson, E., Rodenbeck, C., Seferian, R., Schwinger, J., Smith, N., Tans, P. P., Tian, H., Tilbrook, B., Tubiello, F. N., van der Werf, G. R., Wiltshire, A. J.,

425   and Zaehle, S.: Global Carbon Budget 2019, Earth System Science Data, 11, 1783-1838, 10.5194/essd-11-1783-2019, 2019.

George, K., Ziska, L. H., Bunce, J. A., and Quebedeaux, B.: Elevated atmospheric CO2 concentration and temperature across an urban-rural transect, Atmospheric Environment, 41, 7654-7665, 10.1016/j.atmosenv.2007.08.018, 2007.

Grimmond, C. S. B., King, T. S., Cropley, F. D., Nowak, D. J., and Souch, C.: Local-scale fluxes of carbon dioxide in urban environments: methodological challenges and results from Chicago, Environmental Pollution, 116, S243-S254,

430   10.1016/s0269-7491(01)00256-1, 2002.

Gross, B., Zheng, Z., Liu, S., Chen, X., Sela, A., Li, J., Li, D., and Havlin, S.: Spatio-temporal propagation of COVID-19 pandemics, https://arxiv.org/abs/2003.08382, 2020.

Han, P., Cai, Q., Oda, T., Zeng, N., Shan, Y., Lin, X., and Liu, D.: Assessing the recent impact of COVID-19 on carbon emissions from China using domestic economic data, The Science of the total environment, 750, 141688-141688,

435   10.1016/j.scitotenv.2020.141688, 2020.

Idso, C. D., Idso, S. B., and Balling, R. C.: The urban CO2 dome of Phoenix, Arizona, Physical Geography, 19, 95-108, 10.1080/02723646.1998.10642642, 1998.

Idso, C. D., Idso, S. B., and Balling, R. C.: An intensive two-week study of an urban CO2 dome in Phoenix, Arizona, USA, Atmospheric Environment, 35, 995-1000, 10.1016/s1352-2310(00)00412-x, 2001.

440   Idso, S. B., Idso, C. D., and Balling, R. C.: Seasonal and diurnal variations of near-surface atmospheric CO2 concentration within a residential sector of the urban CO2 dome of Phoenix, AZ, USA, Atmospheric Environment, 36, 1655-1660, 10.1016/s1352-2310(02)00159-0, 2002.

Khan, A., Schaefer, D., Tao, L., Miller, D. J., Sun, K., Zondlo, M. A., Harrison, W. A., Roscoe, B., and Lary, D. J.: Low Power Greenhouse Gas Sensors for Unmanned Aerial Vehicles, Remote Sensing, 4, 1355-1368, 10.3390/rs4051355, 2012.

445   Le Quere, C., Jackson, R. B., Jones, M. W., Smith, A. J. P., Abernethy, S., Andrew, R. M., De-Gol, A. J., Willis, D. R., Shan, Y., Canadell, J. G., Friedlingstein, P., Creutzig, F., and Peters, G. P.: Temporary reduction in daily global CO2 emissions during the COVID-19 forced confinement, Nature Climate Change, 10.1038/s41558-020-0797-x, 2020.

LI-COR LI-7810 Brochure, access: 20Jun2020, 2019.

Liu, Z., Ciais, P., Deng, Z., Lei, R., Davis, S., Feng, S., Zheng, B., Cui, D., Dou, X., He, P., Zhu, B., Lu, C., Ke, P., Sun, T., Wang, Y.,

450   Yue, X., Wang, Y., Lei, Y., Zhou, H., Cai, Z., Wu, Y., Guo, R., Han, T., Xue, J., Boucher, O., Boucher, E., Chevallier, F., Wei, Y., Zhong, H., Kang, C., Zhang, N., Chen, B., Xi, F., Marie, F., Zhang, Q., Guan, D., Gong, P., Kammen, D., He, K., and Schellnhuber, H.: COVID-19 causes record decline in global CO2 emissions, https://arxiv.org/abs/2004.13614, 2020.

Martin, C. R., Zeng, N., Karion, A., Dickerson, R. R., Ren, X., Turpie, B. N., and Weber, K. J.: Evaluation and environmental correction of ambient CO2 measurements from a low-cost NDIR sensor, Atmospheric Measurement Techniques, 10,

455   2383-2395, 10.5194/amt-10-2383-2017, 2017.

Mitchell, L. E., Lin, J. C., Bowling, D. R., Pataki, D. E., Strong, C., Schauer, A. J., Bares, R., Bush, S. E., Stephens, B. B., Mendoza, D., Mallia, D., Holland, L., Gurney, K. R., and Ehleringer, J. R.: Long-term urban carbon dioxide observations reveal spatial and temporal dynamics related to urban characteristics and growth, Proceedings of the National Academy of Sciences of the United States of America, 115, 2912-2917, 10.1073/pnas.1702393115, 2018.

460   Mueller, M., Graf, P., Meyer, J., Pentina, A., Brunner, D., Perez-Cruz, F., Huglin, C., and Emmenegger, L.: Integration and calibration of non-dispersive infrared (NDIR) CO2 low-cost sensors and their operation in a sensor network covering Switzerland, Atmospheric Measurement Techniques, 13, 3815-3834, 10.5194/amt-13-3815-2020, 2020.

Perez, I. A., Luisa Sanchez, M., Angeles Garcia, M., and de Torre, B.: CO2 transport by urban plumes in the upper Spanish plateau, Science of the Total Environment, 407, 4934-4938, 10.1016/j.scitotenv.2009.05.037, 2009.

465   Picarro G2401 Analyzer Datasheet access: 20jul2020, 2017.

Picarro G2301 Analyzer Datasheet, access: 20Jun2020, 2019.

Atmospheric
Chemistry
and Physics
Discussions

Rosenzweig, C., Solecki, W., Hammer, S. A., and Mehrotra, S.: Cities lead the way in climate-change action, Nature, 467, 909-911, 10.1038/467909a, 2010.

SenseAir: K30 products sheets, access: 20jul2020, 2019.

470 Shusterman, A. A., Teige, V. E., Turner, A. J., Newman, C., Kim, J., and Cohen, R. C.: The BErkeley Atmospheric CO2 Observation Network: initial evaluation, Atmospheric Chemistry and Physics, 16, 13449-13463, 10.5194/acp-16-13449-2016, 2016.

Sun, W., Deng, L., Wu, G., Wu, L., Han, P., Miao, Y., and Yao, B.: Atmospheric Monitoring of Methane in Beijing Using a Mobile Observatory, Atmosphere, 10, 10.3390/atmos10090554, 2019.

475 Sussmann, R., and Rettinger, M.: Can We Measure a COVID-19-Related Slowdown in Atmospheric CO2 Growth? Sensitivity of Total Carbon Column Observations, Remote Sensing, 12, 10.3390/rs12152387, 2020.

Woodwell, G. M., Houghton, R. A., and Tempel, N. R.: ATMOSPHERIC CO2 AT BROOKHAVEN, LONG-ISLAND, NEW-YORK - PATTERNS OF VARIATION UP TO 125 METERS, Journal of Geophysical Research, 78, 932-940, 10.1029/JC078i006p00932, 1973.

480 Zeng, N., Zhao, F., Collatz, G. J., Kalnay, E., Salawitch, R. J., West, T. O., and Guanter, L.: Agricultural Green Revolution as a driver of increasing atmospheric CO2 seasonal amplitude, Nature, 515, 394-+, 10.1038/nature13893, 2014.

Analysis of road traffic operation in Beijing during COVID-19 in 2020, access: 31Aug2020, 2020.

Zhang, Z., Wong, M., and Lee, K.: Estimation of potential source regions of PM2.5 in Beijing using backward trajectories, Atmospheric Pollution Research, 6, 173-177, 10.5094/apr.2015.020, 2015.

485 Zheng, J., Dong, S., Hu, Y., and Li, Y.: Comparative analysis of the CO2 emissions of expressway and arterial road traffic: A case in Beijing, Plos One, 15, 10.1371/journal.pone.0231536, 2020.